DOI: https://doi.org/10.53350/pjmhs22168614

ORIGINAL ARTICLE

Synthesis, Characterization, and Biological Activity of Mixed ligand Complexes from 8-Hydroxyquinoline and new Ligand for β-Enaminone

MAYSAM B. ABDULSALAM[1], AHMED T. NUMAN[1]
[1]Department of Chemistry, College of Education for Pure Sciences, Ibn-Al-Haitham , University of Baghdad , Baghdad , Iraq
Correspondence to: Maysam B. Abdulsalam, Email: maysambasem86@gmail.com

ABSTRACT

The synthesized ligand [4-chloro-5-(N-(5,5-dimethyl-3-oxocyclohex-1-en-1-yl)sulfamoyl)-2-((furan-2-ylmethyl)amino)benzoic acid] (H_2L_1) was identified utilizing Fourier transform infrared spectroscopy (FT-IR), ^{1} H, ^{13} C – NMR, (C.H.N), Mass spectra, UV-Vis methods based on spectroscopy. To detect mixed ligand complexes, analytical and spectroscopic approaches such as micro-analysis, conductance, UV-Visible, magnetic susceptibility, and FT-IR spectra were utilized. Its mixed ligand complexes [$M(L_1)(Q)Cl_2$] [where M= $Co^{(II)}$, $Ni^{(II)}$, and $Cd^{(II)}$] and complexes [$Pd(L_1)(Q)$] and [$Pt(L_1)(Q)Cl_2$]; [H_2L_1] =β-enaminone ligand =L_1 and Q= 8-Hydroxyquinoline = L_2]. The results showed that the complexes were synthesised utilizing the molar ratio M: L_1:L_2 (1 :1 :1). The formation of six-coordinate octahedral geometry was proposed for metal complexes Co (II), Ni (II), Cd (II), and Pt (IIII), while the Pd (II) complex was square planar. By using the agar well diffusion method, the ligands and complexes were evaluated for antibacterial activity against Staphylococcus aureus, Escherichia coli. The studies demonstrate that the ligand and its complexes have variable activity against the bacterial types, Some of the complexes had an effect on bacteria, while others had less inhibitory action than the ligand. Also, the produced ligand and its metal complexes have been tested for fungi (Candida albicans);the complexes exhibited suppressing activity against fungi compared to the ligand prepared from them.

Keywords: β-enaminones, 5,5-dimethylcyclohexane-1,3-dione , Furosemide, Mixed-ligand complexes, 8-Hydroxyquinoline.

INTRODUCTION

β-Enaminones are chemical compounds that are consisting of an amino group that is connected to a carbonyl group via a C=C bond. Because they possess both the ambident electrophilicity of enones and the ambident nucleophilicity of enamines, they are versatile synthetic intermediates. Typical push-pull ethylenes have an amine group pushing and a carbonyl group pulling on the electron density.

The carbonyl group conjugated to the enamine moiety provides sufficient stability for this system to be easily prepared, isolated and stored at room temperature under atmospheric conditions[1] ,therefore, They have also been made use of as starting materials for the synthesis of anti-inflammatory, antibacterial, anticonvulsant and antitumor agents[2], as well as in the production of naturally occurring alkaloids. The significant advantages of enaminone derivatives are their stability under simulated physiological pH conditions and low level of toxicity [3]. The conjugated system of β- enaminone function is regarded as a functional group in the drug industry. Enaminones produced from β -carbonyl molecules are relatively stable, most likely owing to keto-enol and imine-enamine tautomeric equilibrium[4] (Figure 1). Notably, the structure of the molecule shows that there is a strong intramolecular hydrogen bond along the heterodienic O=C–C=C–NH moiety, which takes the shape of a six-membered ring and makes the structure stiffer[5].

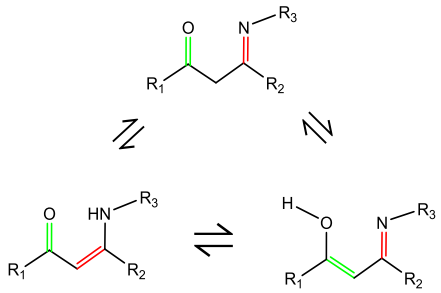

Figure 1: Tautomeric equilibria of β- enaminones.

5,5-dimethylcyclohexane-1,3-dione, is an organic compound that belongs to the cyclic ß-diketones type[6]. These white to light yellow crystalline are also known as methone, dimethyldihydroresorcinol, and cyclomethone. The melting point of $C_8H_{12}O_2$ (M.wt = 140.179 g/mol) is 147-150 °C (420-423 K). Its stable in ambient conditions and soluble ethanol, methanol, and water as well as inorganic solvents[7],[8]. It is one of the most prominent cyclic 1,3-dicarbonyls, and its uses may be found in a variety of fields, including industrial, synthetic organic chemistry, and analytical chemistry[9].

Furosemide(Fur) chemical name is 4-chloro-2-[(2-furanylmethyl)-amino]-5-sulfamoylbenzoic acid [10],[11].It is known by the generic names Fursemide, Lasix[12]. It is a loop diuretic with a high ceiling that is used to treat edema and hypertension associated with congestive heart failure, renal disease and cirrhosis of the liver[13],[14]. Its molecule includes potential hydrogen bond donor and acceptor groups :-SO_2NH_2 , NH and COOH[15].

mixed ligand complexes play a significant role when it comes to the activation of enzymes. The biological activity of mixed ligand complexes against pathogenic bacteria has been explored . N- and O- donor ligands were utilized in the production of metal complexes to study a variety of antifungal and antimicrobial activities[16],[17]. Organic bi-dentate ligands have been the most important class of ligands in coordination chemistry, and they have numerous applications in various fields. The ligands are composed of donor atoms such as nitrogen, oxygen, and carbonyl groups. Consequently, its own interaction with metal ions results in the formation of complexes with different geometries that are biologically active. In latest years, mixed ligand transition metal complexes have gained prominence. These complexes have been studied for their utility in various fields. Some metal ligand complexes catalyzed oxidation, oxidative cleavage , reduction, etc. [18],[19]. It is well established that mixed ligand chelates play an important role in biological processes such as the activation of enzymes, storage, and transport of substances across membranes[20].

8-Hydroxyquinoline is a white to off-white crystal or powder that is insoluble in water but freely soluble in aqueous mineral acids , acetone, ethanol, and chloroform[21]. The chemical compound 8-Hydroxyquinoline (8-HQ , quinolin-8-ol, C_9H_7NO, oxine)[22],[23]. 8-HQ is a conjugated system and a bifunctional hydrogen bonding molecule that, in protic solvents, acts as a H acceptor at the N atom and as H donor at the O-H group simultaneously . A keto-enol tautomeric equilibrium may also involve the O-H and aza groups. Due to a short distance between the ring N atom and the OH group[24- 29].

Experimental

Chemicals: Every chemical used was analytical grade, and it had not been further purified before usage.

Analytical and physical measurements: Shimadzu (FT-IR)-8300 Infrared Spectrophotometer was used to record FT-IR spectra in the (4000–400) cm–1 range. Spectra were recorded on potassium

bromide (KBr) discs as well as through CsI discs in the range of 400-200 cm-1 registered on Shimadzu 8400s FT-IR. The Electro-thermal Stuart (SMP40) was utilized to Melting point measurement. Electronic spectra were recorded from (200-1100 nm) for 10^{-3} M solutions in DMSO at room temperature using a Shimadzu 1800 [UV-Vis] spectrophotometer with a quartz cell of 1.00 cm length. Microanalysis (C.H.N) analyzer on a Heraeus instrument (Vario EL) was used to measure elemental microanalyses. The amount of chloride that is present in complexes was measured utilizing a potentiometric titration technique using a [686-Titro Processor-665. Dosimat Metrohm Swiss]. Magnetic moments (μ_{eff} B.M)were determined utilizing a magnetic susceptibility balance (Sherwood-Scientific). The ^{1}H-NMR spectra of the ligands were determined in DMSO-d^6 as a solvent, Utilizing tetramethylsilane (TMS) as an internal standard on Agilent Technologies-500 MHz spectrometer. Chemical shifts are measured in ppm downfield from the TMS reference. Electrospray mass spectroscopy was utilized to determine the ligands in the positive mode on the Agilent Sciex ESI- MS. The metal ratios of the complexes were determined with the help of the atomic absorption (A.A) technique. This was done with an atomic absorption spectrophotometer made by Shimadzu (model A.A 680 GBC 933 plus).

Synthesis of the ligand [H_2L_1]: A 5,5-dimethylcyclohexane-1,3-dione (0.105g , 0.749 mmole) was dissolved in absolute benzene 10mL with a few drops of glacial acetic acid were added with constant stirring , Then Furosemide (0.25 g, 0.75mmol) dissolved in 25 mL absolute benzene with a few drops of DMSO were added with continual stirring . The solutions were mixed in a round bottom flask 100mL , The mixture was then stirred continuously until it converted into a light yellow solution. The resulting solution was refluxed for 7 hours until the light yellow precipitate was noted, TLC was used to monitor the reaction. At room temperature, the reaction mixture was allowed to cool . The light yellow precipitate had a weight of 0.27 g , Yield = % 79.4 , M.P = 162°C ,Scheme (1).

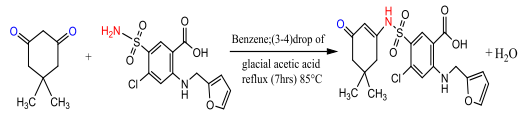

5,5-di-methylcyclohexane-1,3-dione *Furosemide* *[H_2L_1]*

[H_2L_1]= 4-chloro-5-(*N*-(5,5-dimethyl-3-oxocyclohex-1-en-1-yl)sulfamoyl)-2-((furan-2-ylmethyl)amino)benzoic acid

Scheme 1: Synthetic route for the ligand [H_2L_1].

Synthesis of Mixed Ligand Metal Complexes: The metal solution of $CoCl_2.6H_2O$ (0.078 g, 0.33 mmole) in 5 mL of ethanol was stirred for 10 minutes. The ligand solution [H_2L_1] (0.15 g, 0.33 mmole) in 15 mL of ethanol after being adjusted to pH = 8 utilizing a few drops of potassium hydroxide solution was added to the metal solution. In addition, (0.0479 g, 0.33 mmole) 8-Hydroxyquinoline in 5 mL of ethanol was added to the metal solution described above. The resultant mixture was heated for 4 hours under reflux conditions. A solid complex was formed, It was collected by filtration and dried for 24 hours at ambient temperature. An olive solid was obtained. Weight (0.19 g), Yield = (70.3 %), M.P = (>270)°C. The method utilized to prepare the complexes of [Ni^{II}], [Cd^{II}], [Pd^{II}] and [Pt^{IIII}] ions was a similar approach to that described in the section on the preparation of the [Co^{II}] complex (Figure 2) . The micro-analysis of results and a few physical characteristics for ligand(H_2L_1) and the prepared complexes in Table (1).

Table 1: The micro-analysis of results and a few physical characteristics for ligand(H_2L_1) and the prepared complexes.

No	Compounds	Color	M.P (°C)	M.Wt g.mol^{-1}	Yield (%)	Elemental analysis found (Calc.)				Molar conductivity (S.cm^2 molar $^{-1}$)
						C	H	N	M	
1	[H_2L_1]	Light Yellow	162	452.9	9.4	53.04 52.84	4.67 4.46	6.19 6.39		
2	K_2[$Co(L_1)(Q)Cl_2$]	Olive	>270	842.2	70.3	41.36 41.73	2.99 3.18	4.99 4.81	6.99 7.37	9.59
3	K_2[$Ni(L_1)(Q)Cl_2$]	Pale Green	>270	41.9	82.01	41.36 40.91	2.99 2.65	4.99 4.78	6.96 6.54	11.17
4	K_2 [$Cd(L_1)(Q)Cl_2$]	Yellow	>270	95.7	60.81	38.89 39.02	2.81 2.66	4.69 4.3	12.55 12.73	4.09
5	[$Pd(L_1)(Q)$]	Brown	>270	40.6	66.93	47.03 47.5	3.40 3.88	5.67 5.24	14.37 13.58	16.12
6	[$Pt(L_1)(Q)Cl_2$]	Olive	220	00.1	59.73	38.70 39.1	2.80 2.63	4.67 4.22	21.65 22.39	12.32

* decompose

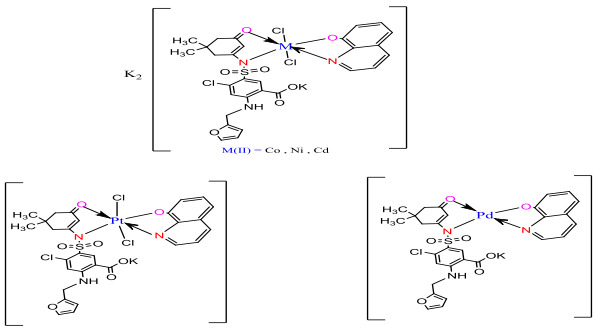

Figure 2: The suggested chemical structure of the complexes.

RESULTS AND DISCUSSION

FT- IR Spectral data for ligand [H_2L_1] , 8-HQ and K_2[$Co(L_1)(Q)Cl_2$] ①, K_2[$Ni(L_1)(Q)Cl_2$]② , [$Pd(L_1)(Q)$]③, K_2[$Cd(L_1)(Q)Cl_2$]④ and [$Pt(L_1)(Q)Cl_2$]⑤ complexes: As shown in Fig. (3), the (N-H) stretching vibration is responsible for the sharp band at (3375) cm^{-1}, and the (N-H) enaminone is responsible for the band at (3251) cm^{-1} and υ(O - H) is responsible for the stretching band at (3498) cm^{-1}. It was determined that the $\upsilon(C\text{-}H)_{aroma.}$ stretching vibrations were responsible for the band at (3082) cm^{-1}. The stretching band $\upsilon(C\text{-}H)_{aliph.}$ is responsible for the bands detected at (2958)cm^{-1} and (2873) cm^{-1}. The bands at (1681) cm^{-1} and (1616)cm^{-1} were attributed to $(C=O)_{dim.}$ and $(C=O)_{carb.}$ stretching vibrations respectively. The stretching bands $\upsilon_{asy}(S=O)$ and $\upsilon_{sy}(S=O)$ are responsible for the bands detected at (1346) cm^{-1} and (1165) cm^{-1}[30],[31]. The stretching band υ(C=N) is responsible for the band detected at (1577)cm^{-1}[32]. As well as the stretching band at (1562) cm^{-1} allotted to υ(C=C).Finally, the stretching band at (1242) cm^{-1} was attributed to υ(C-N) stretching vibration[33]. Also spectrum for 8-Hydroxyquinoline show a band at (3479) cm^{-1} is attributable to υ(O−H) stretching vibration . The bands at (3182) and (3047) cm^{-1} were allotted to $\upsilon(C-H)_{aroma.}$ stretching vibration. In addition, the band at (1577) cm^{-1} was allotted to the υ(C=N) stretching vibration. Finally, the υ(C=C) stretching vibration appears at (1504)cm^{-1} [34-37] .

The attribution of the characteristic bands in the FT-IR spectrum for the ligand [H_2L_1] and its complexes is described in table (2). The ligand [H_2L_1] contains an (N-H) secondary amine group at (3375) cm$^{-1,}$ which remained in the complexes and had frequencies at (3414), (3387), (3379), (3417), and (3379), while the

band at (3251) cm^{-1} in the FT-IR spectrum of the ligand $[H_2L_1]$ caused by the (N-H) enaminone stretching vibration indicates that the ligand is loose. Moreover, the band disappearance of the hydroxyl group at(3498)cm^{-1} in all complexes is due to the replacement of the potassium ion coming from potassium hydroxide in place of the hydrogen ion in the carboxyl group. As well as, the FT-IR spectra for 8-hydroxyquinoline has a band at (3479) cm^{-1} that is caused by the (O-H) group stretching vibration, but on complexation, these bands disappear for complexes ①, ②, ③, ④, and ⑤ demonstrating that the coordination occurs through the oxygen atom of the hydroxyl group for (8-HQ) and the nitrogen atom of the enamine group for $[H_2L_1]$.

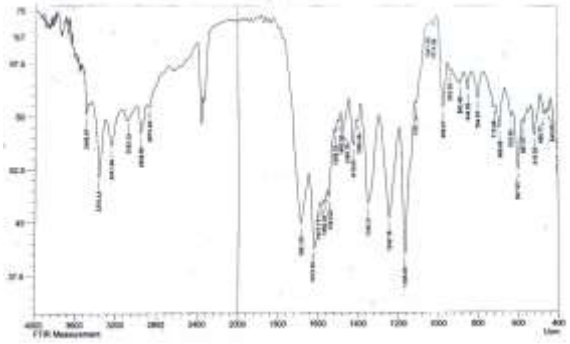

Figure 3: FT - IR spectrum of the ligand $[H_2L_1]$

The band at (1577)cm^{-1} for the (C=N) of 8-hydroxyquinoline , but this band has been shifted to lower frequency at (1500),(1496),(1554), (1539) and (1554)cm^{-1} for complexes ①, ②, ③, ④ and ⑤ respectively , suggesting that the coordination is via the nitrogen atom of the (C=N) group. Because oxygen and nitrogen atoms are coordinated to the metal atom, the carbonyl group $(C=O)_{dim.}$ and the imine group(C=N) have lower frequencies.

In FT-IR complexes, the appearance of new bands at (547, 586), (543, 582), (540, 563), (532, 586) and (540, 563)cm^{-1} were allotted to υ(M-O) for complexes ①, ②, ③, ④,and ⑤ indicating that to the oxygen of ligands are included in coordination with metals ions. In addition, υ (M-N) was assigned to the appearance of new bands at (412, 447), (459, 459), (432, 459), (432, 459) and (432, 459)cm^{-1} for ①, ②, ③, ④ and ⑤Complexes[38],[39].

At lower frequencies (far - IR) of the complexes, the appearance of new bands at (368, 351), (372, 351), (381, 351) and (378, 349) cm^{-1} were allotted to υ(M-Cl) for ①,②,④,⑤ complexes[40-42]. The FT-IR spectra for complex $Cd^{(II)}$ shown in Figure (4).

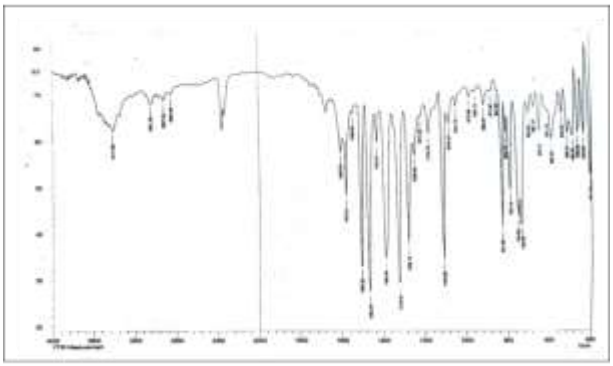

Figure 4: FT-IR spectrum of $K_2[Cd(L_1)(Q)Cl_2]$.

Table 2: FT- IR spectral data (wave number) cm^{-1} of $[H_2L_1]$, (8-HQ), K_2 $[Co(L_1)(Q)Cl_2]$① ,$K_2[Ni(L_1)(Q)Cl_2]$②, $[Pd(L_1)(Q)]$③, $K_2[Cd(L_1)(Q)Cl_2]$④ and $[Pt(L_1)(Q)Cl_2]$⑤

Compounds	$[H_2L_1]$	8-HQ	(1)	(2)	(3)	(4)	(5)
υ(N-H)	3375 3251		3414	3387	3352	3417	3379
$υ(C=O)_{carb.}$ $υ(C=O)_{dim.}$	1685 1616		1604 1577	1608 1577	1708 1600	1600 1573	1708 1600
$υ(C-H)_{aliph.}$	2958 2873		2962 2870	2958 2889	2958 2893	2927 2854	2962 2893
$υ(C-H)_{arom.}$	3082	3182 3047	3047	3047	3062	3051	3089
υ(C-N)	1242	1222	1269	1265	1234	1269	1234
υ(C=N)	1577	1577	1500	1558	1554	1539	1577
υ(C=C)	1562	1562	1465	1465	1469	1462	1469
$υ_{asy}(S=O)$ $υ_{sy}(S=O)$	1346 1165		1381 1165	1377 1161	1369 1165	1384 1127	1373 1165
υ(O-H)	3498	3479					
υ(M-N)			412 447	459 459	432 459	432 459	432 459
υ(M-O)			547 586	543 582	540 563	532 586	540 563
υ(M-Cl)			368 351	372 351		381 351	351 368

Table 3: ^{1}H-NMR spectrum data for the precursor $[H_2L_1]$.

Compound	Functional groups	δ (ppm)
$[H_2L_1]$	(O-H) carboxylic acid	13.16
	$(C_{16}$ -NH) Enaminone group	8.65
	N-H For (C_8 –NH) group	8.41
	(C_4 , C_7) For (Ar-H)	8.36 , 7.11
	(C_{10})For CH_2 group	4.63
	(C_{12} ,C_{13}, C_{14}) For CH group of the furan	6.42 , 6.38 , 7.11
	(C_{17}) For CH group	5.21
	(C_{19},C_{21}) For CH_2 groups	2.13, 2.29
	(C_{22}) For CH_3 groups	0.99 , 1.03
	DMSO Solvent	2.5

Nuclear magnetic resonance spectra of the ligand $[H_2L_1]$: ^{1} H-NMR spectra of the ligand $[H_2L_1]$

Figure (5) represents the ^{1}H-NMR spectrum of $[H_2L_1]$.The spectrum shows the singlet signal at (δ = 13.16 ppm) is assigned to the (O-H) proton of carboxylic acid group[43],[44], the singlet signal at (δ = 8.6 ppm) is attributed to the one proton for (N-H) enamine group of (S-NH), and the singlet signal at (δ = 8.41 ppm) is allotted to the proton for the (N-H) of (C_8-NH) secondary amine. The aromatic signals in the $[H_2L_1]$ spectra are single chemical shifts at (δ=8.36ppm) ,(δ= 7.11ppm) and are assigned to protons of (C_4) and (C_7) aromatic ring [45],[46]. Table(3) provides a summary of all of these references.

^{13}C-NMR spectrum for the precursor $[H_2L_1]$: The ^{13}C-NMR spectrum of $[H_2L_1]$. In the middle of the DMSO-d^6 solvent, as depicted in Figure (6), the first carbonyl group $(C=O)_{dim.}$ for an aliphatic ring was detected around (δ=169.09 ppm). The carbonyl group$(C=O)_{carb.}$ for aromatic ring observed around (δ=168.82 ppm).

The chemicals shifts at (δ=152.83 ppm) and (δ = 151.79ppm)allotted to C_8 for (C_8-NH) group and C_{16} for (C_{16}-NH) respectively[47],[48]. Multiples chemical shifts at (δ=133.78 - 110.99 ppm) range are allotted to (C_6, C_5, C_4, C_7) for aromatic ring[49]. The chemical shifts at (δ= 143.17 ppm), (δ= 136.66 ppm), (δ= 108.62 ppm) and (δ= 108.09 ppm) were assigned to C_{14} , C_{11} , C_{12} ,C_{13} respectively for the furan ring .The chemical shift at (δ= 102.90 ppm) to C_3 for (C_3-CO) and C_{17} for (C_{17}-CO). The chemical shifts at (δ= 40.88ppm) were attributed to C_{10} , C_{19} and C_{21} for the CH_2 groups. The chemical shift to DMSO solvent occurs at (δ= 39.97 ppm) . The chemical shift at (δ= 32.58 ppm) refers to C_{20} for aliphatic ring. Finally, The carbon atoms C_{22} of CH_3 groups resonated with the chemical shifts at (δ = 28.41 ppm)[50],[51] . Table(4) gives a brief summary of the results.

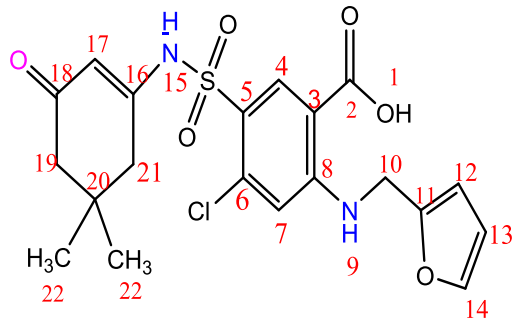

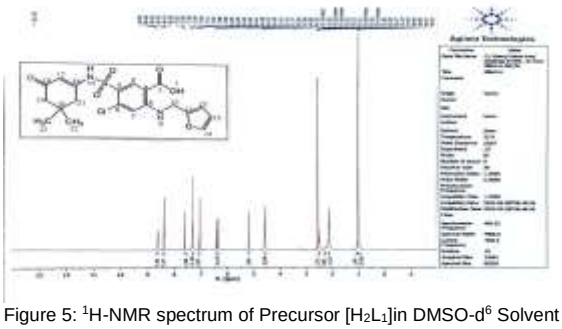

Figure 5: ^{1}H-NMR spectrum of Precursor [H_2L_1]in DMSO-d^6 Solvent

Table 4: ^{13}C-NMR spectrum data for precursor [H_2L_1] .

Compound	Functional groups	δ (ppm)
[H_2L_1]	$(C=O)_{dim.}$ for aliphatic ring	169.09
	$(C=O)_{carb.}$ for aromatic ring	168.82
	C_8-NH for aromatic ring	152.83
	C_{16}-NH (enaminone)	151.79
	C_{14} for C-O of the furan ring	143.17
	C_{11} for C-O of the furan ring	136.66
	C_6 ,C_5 for aromatic ring	133.78 , 127.28
	C_4 ,C_7 for CH of the aromatic ring	114.02, 110.99
	C_{13} ,C_{12} for CH of the furan ring	108.62 , 108.09
	C_3-CO , C_{17}-CO groups	102.90
	C_{10} ,C_{19},C_{21} for CH_2 of the aliphatic ring	40.88
	C_{20} for aliphatic ring	32.58
	C_{22} For methyl groups	28.41

Mass spectrum of the Precursor [H_2L_1]: Positive ESI-MS for [H_2L_1] is seen in Figure (7). There was no peak visible on the spectrum at m/z = 452, may be attributable to the parent compound's molecular ion [M-H]$^+$. While the peak appeared at 450 which could be attributed to [M^{-2}]$^+$ [52].As well as appearance of the peak at m /z = 407, which can be traced to [$C_{19}H_{20}ClN_2O_5S$]$^{+\cdot}$ Resulted from the fragment of the carboxyl group included in the ligand. The pattern of fragmentation of [H_2L_1] is shown in Table (6)

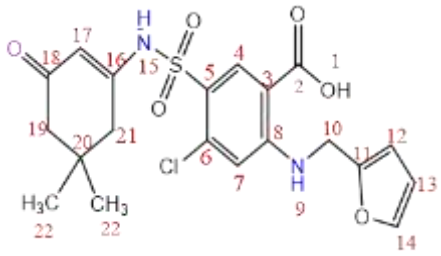

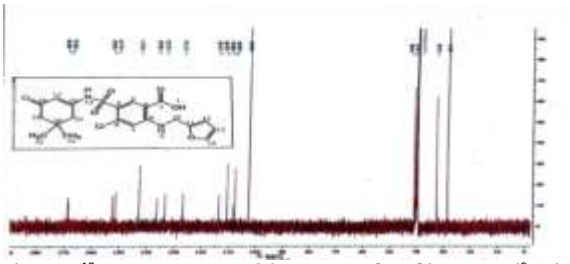

Figure 6: ^{13}C-NMR spectrum of the precursor[H_2L_1] in DMSO-d^6 Solvent.

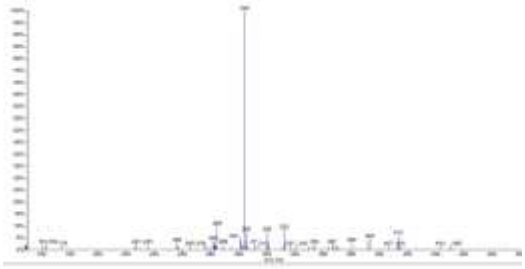

Figure 7: ESI (+) mass spectrum of the precursor [H_2L_1].

Table 6: A Fragmentation pattern belonging to[H_2L_1].

Fragment	MASS / Charge (m / z)
[$C_{20}H_{21}ClN_2O_6S$]$^+$	Not detected
[$C_{19}H_{20}ClN_2O_4S$]$^{+\cdot}$	407
[$C_{17}H_{13}ClN_2O_5S$]$^{+\cdot}$	393
[$C_{14}H_{11}ClN_2O_5S$]$^{+\cdot}$	354
[$C_{14}H_{12}ClNO_5S$]$^{+\cdot}$	341
[$C_{14}H_{14}ClNO_3S$]$^{+\cdot}$	311
[$C_{11}H_6ClO_5S$]$^{+\cdot}$	285
[$C_{10}H_6ClNO_3S$]$^{+\cdot}$	256
[$C_{11}H_8NO_3S$]$^{+\cdot}$	234
[$C_{10}H_{13}NO_3S$]$^{+\cdot}$	227
[C_5H_5O]$^{+\cdot}$	81

UV-Vis spectra of ligand [H_2L_1],8-HQ and their metal complexes: Table (7) gives the UV-Vis spectra of [H_2L_1] , 8-HQ and their complexes $K_2[Co(L_1)(Q)Cl_2]$ ①, $K_2[Ni(L_1)(Q)Cl_2]$②, $[Pd(L_1)(Q)]$③, $K_2[Cd(L_1)(Q)Cl_2]$④ and $[Pt(L_1)(Q)Cl_2]$⑤ complexes that measured in DMSO, in the range (200-1000) nm Figures (7) and (8) Electronic spectrum of K_2 $[Cd(L_1)(Q)Cl_2]$ and $[Pt(L_1)(Q)Cl_2]$ complexes.

Table 7:

Compound	Wave number		ε_{max} molar^{-1}.cm^{-1}	Assignment	μ_{eff} (B.M)	Suggested structure
	nm	cm^{-1}				
[H_2L_1]	272 345	36764.7 28985.5	1863 1909	π → π* n → π*		
8-HQ	279 324	35842.2 30864.1	2213 1232	π → π* n → π*		
①	271	36900.3	1774	L.F	4.76	distorted

	345 402 689 766 806	28985.5 24875.6 14513.7 13054.8 12406.9	1172 938 56 56 54	L.F C.T $^4T_1g_{(F)} \rightarrow {}^4T_1g_{(P)}$ $^4T_1g_{(F)} \rightarrow {}^4A_2g_{(F)}$ $^4T_1g_{(F)} \rightarrow {}^4T_2g_{(F)}$		octahedral
②	273 344 393 760 925	36630 29069.7 25445.2 13157.8 10810.8	2046 2060 1630 14 12	L.F L.F C.T $^3A_2g_{(F)} \rightarrow {}^3T_1g_{(F)}$ $^3A_2g_{(F)} \rightarrow {}^3T_2g_{(F)}$	3.08	Distorted octahedral
③	270 301 348 711 797	37037 33222.5 28735.6 14064.9 12547	1557 1554 1120 22 22	L.F L.F C.T $^1A_1g \rightarrow {}^1E_1g$ $^1A_1g \rightarrow {}^1B_1g$		Square planar
④	273 328 393	36630 30487.8 25445.2	2041 1063 591	L.F L.F C.T		Distorted octahedral
⑤	269 348 363 688	37174.7 28735.6 27548.2 14534.8	1405 863 1212 19	L.F L.F C.T $^1A_1g \rightarrow {}^3T_2g$		Distorted octahedral

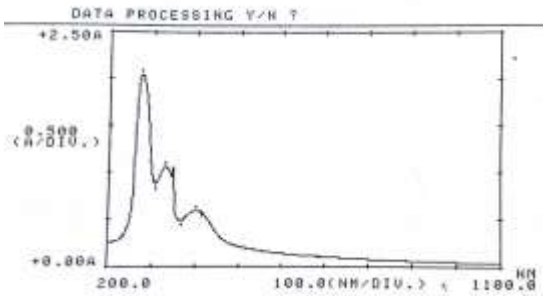

Figure 7: Electronic spectrum of K_2 [Cd(L_1)(Q)Cl_2].

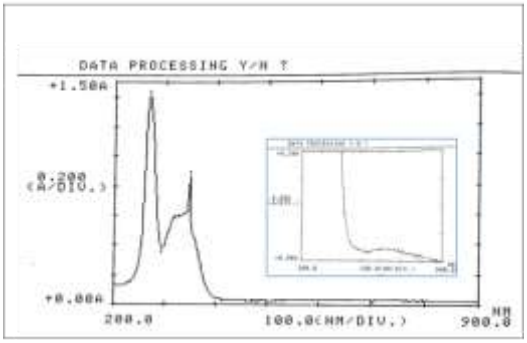

Figure 8: Electronic spectrum of [Pt(L_1)(Q)Cl_2]

Biological activity for the ligand [H_2L_1],8-Hydroxyquinoline and their complexes K_2[Co(L_1)(Q)Cl_2]①, K_2[Ni(L_1)(Q)Cl_2]②, [Pd(L_1)(Q)]③ , K_2[Cd(L_1)(Q)Cl_2]④ , [Pt(L_1)(Q)Cl_2]⑤: The biological activity of the ligand [H_2L_1] and a number of its metal complexes ①, ②, ③, ④ and ⑤,were tested for their antibacterial activity against Staphylococcus aureus which is a Gram-positive bacteria, and Escherichia coli, which is a Gram-negative bacteria, as well as the fungi (Candida albicans).

The following conclusions are drawn from the information recorded and displayed in the Table (8)

1- Using the concentration (10^{-2}M):-

A- Escherichia coli :- The ligand [H_2L_1] and the complex ③ displayed similar activity in inhibiting Escherichia coli compared to the rest of the complexes. At varying rates, the Complexes inhibited testing bacteria, with ③ >② >① > ④ = ⑤ being the sequence of decreasing activity.

B- Staphylococcus aureus:- The complex ② showed a higher activity in inhibiting Staphylococcus aurous than the rest of the same ligand complexes and the ligand [H_2L_1]. The Complexes inhibited testing bacteria at varied rates, with ②>③ =④ > ⑤ > ① the order of decreasing activity being . complex① showed similar inhibition to the ligand [H_2L_1].

C- Candida albicans :- The complex ③ offered a higher activity in inhibiting of Candida albicans than the rest of the same ligand complexes and the ligand [H_2L_1]. The Complexes inhibited testing the fungi at varied rates, with ③ > ① >②>⑤ >④ the order of decreasing activity being. For information, Complex ④showed less inhibitory activity than the ligand [H_2L_1]

2- Utilizing the concentration (10^{-3}M):-

A- Escherichia coli :- The ligand [H_2L_1] revealed that higher activity in inhibiting of Escherichia coli compared of their complexes. The Complexes inhibited tested bacteria at varying rates, with ① = ⑤ >③ = ④ >② being the sequence of decreasing activity. Complexes②& ③&④ showed less inhibitory activity than the ligand [H_2L_1]

B- Staphylococcus aureus:- The complex ① displayed a higher activity in inhibiting of Staphylococcus aureus than the rest of the same ligand complexes and the ligand [H_2L_1]. At varying rates, the Complexes inhibited testing bacteria, with ① > ②= ③ = ④ > ⑤ the order of decreasing activity being.

C- Candida albicans :- The ligand [H_2L_1] and the complex ①,③ and④ displayed similar activity in inhibiting of Candida albicans. The Complexes inhibited testing the fungi at varied rates, with ① = ③ = ④ > ② > ⑤ the order of decreasing activity being.

The reason why some complexes have inhibiting is likely the increased lipophilicity of the complexes. This increased activity of metal complexes could be explained by Overton's theory and Chelation theory . The positive charge of the metal in the chelated complex is partially probably shared with the ligand donor atoms, resulting in electron delocalization throughout the entire chelate ring. This, in turn, enhances the lipophilicity of the metal chelate and facilitates its passage via the lipoid layers of bacterial membranes[53].


Figure 9: The biological activity (Staphylococcus auras) of the mixed-ligand complexes K_2 [Co(L_1)(Q)Cl_2]①, K_2[Ni(L_1)(Q)Cl_2)]②, [Pd(L_1)(Q)]③, K_2[Cd(L_1)(Q)Cl_2)]④ ,[Pt(L_1)(Q)Cl_2]⑤ at concentration (10^{-2}M).

Figure 10: The biological activity (Escherichia coli) of the mixed-ligand complexes K_2 $[Co(L_1)(Q)Cl_2]$①, $K_2[Ni(L_1)(Q)Cl_2)]$②,$[Pd(L_1)(Q)]$③, $K_2[Cd(L_1)(Q)Cl_2)]$④, $[Pt(L_1)(Q)Cl_2]$⑤ at concentration (10^{-2}M)

Figure 11: The biological activity (candida albicans) of the mixed-ligand complexes $K_2[Co(L_1)(Q)Cl_2]$① , $K_2[Ni(L_1)(Q)Cl_2)]$② , $[Pd(L_1)(Q)]$③, $K_2[Cd(L_1)(Q)Cl_2)]$④, $[Pt(L_1)(Q)Cl_2]$⑤at concentration (10^{-2} M).

Figure 12: The biological activity (Staphylococcus auras) of the mixed-ligand complexes K_2 $[Co(L_1)(Q)Cl_2]$①, $K_2[Ni(L_1)(Q)Cl_2)]$②,$[Pd(L_1)(Q)]$③, $K_2[Cd(L_1)(Q)Cl_2)]$④,$[Pt(L_1)(Q)Cl_2]$⑤ at concentration (10^{-3}M).

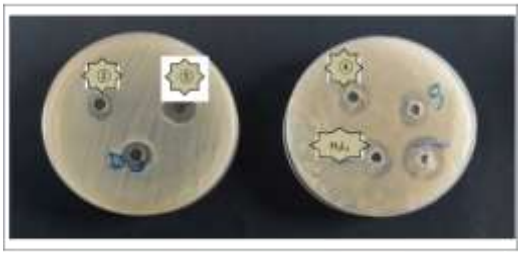

Figure 13: The biological activity (Escherichia coli) of the mixed-ligand complexes where K_2 $[Co(L_1)(Q)Cl_2]$①, $K_2[Ni(L_1)(Q)Cl_2)]$②, $[Pd(L_1)(Q)]$③, $K_2[Cd(L_1)(Q)Cl_2)]$④, $[Pt(L_1)(Q)Cl_2]$⑤ at concentration (10^{-3}M).

Figure 14: The biological activity (candida albicans) of the mixed-ligand complexes K_2 $[Co(L_1)(Q)Cl_2]$①, $K_2[Ni(L_1)(Q)Cl_2)]$②, $[Pd(L_1)(Q)]$③, $K_2[Cd(L_1)(Q)Cl_2)]$④, $[Pt(L_1)(Q)Cl_2]$⑤ at concentration (10^{-3}M).

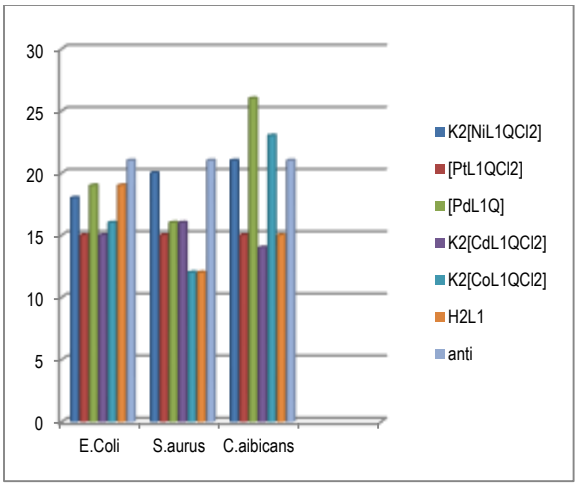

Figure 15: Evolution of $[H_2L_1]$ and its complexes against Candida albicans, E. coli, and S. aureus growth at concentration (10^{-2}M).

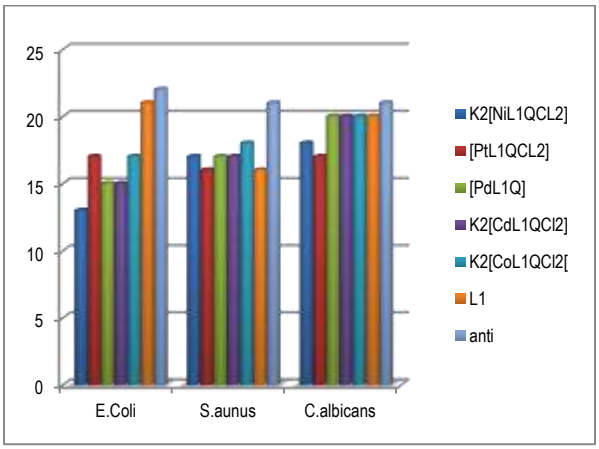

Figure 16: Evolution of $[H_2L_1]$ and its complexes against Candida albicans, E. coli, and S. aureus growth at concentration (10^{-3}M).

Table 8: Inhibition zone diameter in(mm)for the ligand $[H_2L_1]$and their complexes.

Compounds	Escherichia coli		Staphylococcus aureus		Candida albicans	
	10^{-2}M	10^{-3}M	10^{-2}M	10^{-3}M	10^{-2}M	10^{-3}M
$[H_2L_1]$	19	21	12	16	15	20
anti	22	22	21	21	21	21
①	16	17	12	18	23	20
②	18	13	20	17	21	18
③	19	15	16	17	26	20
④	15	15	16	17	14	20
⑤	15	17	15	16	15	17

CONCLUSION

The β-enaminone acted in the form of bidentate ligand through a nitrogen atom in imine (N-H) and oxygen atom in $(C=O)_{dim}$. with the central metal ions M(II): Co, Ni, Pd, Cd also Pt(IIII) with complexes of its general molecular formula: $[M(L_1)(Q)Cl_2]$ and complexes $[Pd(L_1)(Q)]$ and $[Pt(L_1)(Q)Cl_2]$.

For all prepared complexes Co(II), Ni(II), Cd(II), Pt(IIII), the octahedral geometrical structure was recommended while Pd(II) the Square planar geometrical.

REFERENCES

1 Concetta M. K.. (2003). The Chemistry of Enaminones , Diazocarbonyls and Small Rings : Our Contribution. J. Braz. Chem. Soc.

2 Khanikar, S., Kaping, S., Helissey, P., Joshi, P., Shaham, S. H., Mishra, S., Srivastava, M., Tripathi, R., & Vishwakarma, J. N. (2021). Efficient synthesis, structure elucidation, and anti-parasitic activities of novel

quinolinyl β–enaminones. Monatshefte Fur Chemie, 152(6), 665–678. https://doi.org/10.1007/s00706-021-02776-w

3 Prabakaran, K., Sivakumar, M., & Perumal, M. S. (2017). A Simple, Efficient Green Protocol for the Synthesis of β-Enaminone and Enamino Ester Derivatives by Using Onion Extract as Green Catalyst. ChemistrySelect, 2(8), 2363–2372. https://doi.org/10.1002/slct.201601515

4 Bimoussa, A., Oubella, A., Eddine Hachim, M., Youssef Ait Itto, M., Mentré, O., Mostafa Ketatni, E., Bahsis, L., Morjani, H., Auhmani, A., Youssef AIT ITTO, M., Mentre, O., Mostafa KETATNI, E., & Auhmani, andAziz. (n.d.). New enaminone-based to the sesquiterpenic: TiCl4-catalyzed synthesis, spectral characterization, crystal structure, Hirshfeld surface analysis, DFT studies and cytotoxic activity New enaminone-based to the sesquiterpenic skeleton: TiCl4-Catalyzed Synthesis, Spectral Characterization, Crystal Structure,Hirshfeld surface analysis, DFT studies, and cytotoxic activity. https://doi.org/10.1016/j.molstruc.2021.130622ï

5 Chniti, S., Nsira, A., Khouaja, S., Mechria, A., Gharbi, R., Msaddek, M., & Lecouvey, M. (2018). Highly diastereoselective synthesis of rigid 3-enamino-1, 5-benzodiazepines. Arkivoc, 2018(5), 283–295. https://doi.org/10.24820/ark.5550190.p010.426

6 Mohareb, R. M., Manhi, F. M., Mahmoud, M. A. A., & Abdelwahab, A. (2020). Uses of dimedone to synthesis pyrazole, isoxazole and thiophene derivatives with antiproliferative, tyrosine kinase and Pim-1 kinase inhibitions. Medicinal Chemistry Research, 29(8), 1536–1551. https://doi.org/10.1007/s00044-020-02579-4

7 Nikoofar, K., & Yielzoleh, F. M. (2018). A concise study on dimedone: A versatile molecule in multi-component reactions, an outlook to the green reaction media. Journal of Saudi Chemical Society, 22(6), 715–741. https://doi.org/10.1016/j.jscs.2017.12.005.

8 Rao, T. N., Krishnarao, N., Ahmed, F., Alomar, S. Y., Albalawi, F., Mani, P., Aljaafari, A., Parvatamma, B., Arshi, N., & Kumar, S. (2021). One-pot synthesis of 7, 7-dimethyl-4-phenyl-2-thioxo-2,3,4,6,7, 8-hexahydro-1H-quinazoline-5-onesusing zinc ferrite nanocatalyst and its bio evaluation. Catalysts, 11(4). https://doi.org/10.3390/catal11040431

9 Karabulut, S., Namli, H., & Leszczynski, J. (2013). Detection of tautomer proportions of dimedone in solution: A new approach based on theoretical and FT-IR viewpoint. Journal of Computer-Aided Molecular Design, 27(8), 681–688. https://doi.org/10.1007/s10822-013-9669-z

10 Hassouna, M. E. (2016). Spectrophotometric Determination of Furosemide Drug in Different Formulations using Schiff 's Bases. Foresic Research & Criminology International Journal, 1(6). https://doi.org/10.15406/frcij.2015.01.00036

11 McMahon, B. A., & Chawla, L. S. (2021). The furosemide stress test: current use and future potential. In Renal Failure (Vol. 43, Issue 1, pp. 830–839). Taylor and Francis Ltd. https://doi.org/10.1080/0886022X.2021.1906701

12 Saleem, B. A. A., Hamdon, E. A., & Majeed, S. Y. (2021). Visible Quantitative Methods for the Estimation of Furosemide in Pure form and Pharmaceutical Formulations. Journal of Pharmaceutical Research International, 200–209. https://doi.org/10.9734/jpri/2021/v33i47b33113

13 Vlachou, M., Geraniou, E., & Siamidi, A. (2020). Modified release of furosemide from Eudragits® and poly(ethylene oxide)-based matrices and dry-coated tablets. Acta Pharmaceutica, 70(1), 49–61. https://doi.org/10.2478/acph-2020-0010

14 Vlachou, M., Pippa, N., Siamidi, A., & Kyrili, A. (2020). Thermal analysis studies on the compatibility of furosemide with solid state and liquid crystalline excipients. Hemijska Industrija, 74(1), 15–23. https://doi.org/10.2298/HEMIND190910002V

15 Kerr, H. E., Softley, L. K., Suresh, K., Nangia, A., Hodgkinson, P., & Evans, I. R. (2015). A furosemide-isonicotinamide cocrystal: An investigation of properties and extensive structural disorder. CrystEngComm, 17(35), 6707–6715. https://doi.org/10.1039/c5ce01183c

16 Patil, S. S., Thakur, G. A., & Shaikh, M. M. (2011). Synthesis, Characterization, and Antibacterial Studies of Mixed Ligand Dioxouranium Complexes with 8-Hydroxyquinoline and Some Amino Acids. ISRN Pharmaceutics, 2011, 1–6. https://doi.org/10.5402/2011/168539

17 Patil, S. S., Langi, B. P., Gurav, M. N., & Patil, D. K. (2021). Synthesis, Physical and Spectral Investigations and Biological Studies of Mixed Lig and Lanthanum Complexes (Vol. 25). http://annalsofrscb.ro

18 Akter, J., Abu Hanif, M., Masuqul Haque, M., Zahid, M., Saidul Islam, M., Yeamin Reza, M., S Mostofa Zahid, A. A., Kudrat-E-Zahan, M., Akherul Islam, M., & Arjuman Banu, L. (2018). MIXED LIGAND COMPLEXES OF Ni(II) AND Cd(II) WITH PHTHALIC ACID OR SUCCINIC ACID AND HETEROCYCLIC AMINES: SYNTHESIS AND CHARACTERIZATION WITH ANTIMICROBIAL STUDY Evaluation of groundwater quality View project Synthesis, Characterization and Applications of Nanoparticles View project MIXED LIGAND COMPLEXES OF Ni(II) AND Cd(II) WITH PHTHALIC ACID OR SUCCINIC ACID AND HETEROCYCLIC AMINES: SYNTHESIS AND CHARACTERIZATION WITH ANTIMICROBIAL STUDY. https://www.researchgate.net/publication/324209642

19 Nesa, S., Hossain, Md. S., Nasira, S., Uddin, N., Ashrafuzzaman, Md., Habib, Md. A., Rashid, Md. A. M., & Haque, Md. M. (2020). Mixed ligand complexes: Synthesis, characterization and antibacterial activity investigation. International Journal of Chemical Studies, 8(1), 306–312. https://doi.org/10.22271/chemi.2020.v8.i1d.8267

20 Saritha, A., Reddy, C. V. R., & Sireesha, B. (2021). Synthesis, characterization and biological activity of mixed ligand chelates of Ni(II) with pyridoxalthiosemicarbazone and dipeptides. Vietnam Journal of Chemistry, 59(1), 57–68. https://doi.org/10.1002/vjch.202000100

21 Nan, P., Xia, X. H., Du, Q. yan, Chen, J. J., Wu, X. H., & Chang, Z. J. (2013). Genotoxic effects of 8-hydroxylquinoline in loach (Misgurnus anguillicaudatus) assessed by the micronucleus test, comet assay and RAPD analysis. Environmental Toxicology and Pharmacology, 35(3), 434–443. https://doi.org/10.1016/j.etap.2013.02.005

22 Karpińska, G., Mazurek, A. P., & Dobrowolski, J. C. (2011). Hydroxyquinolines: Constitutional isomers and tautomers. Computational and Theoretical Chemistry, 972(1–3), 48–56. https://doi.org/10.1016/j.comptc.2011.06.010

23 Mohammed, S., Obaid, H., Mahdi, W., Hussein, F. H., & Al-Khafaji, Y. (n.d.). Recent Development In Oxine Complexes And Their Medical Application: A Review Investigation of the Photocatalytic for CNT/TiO2/Pt Hydrogen Production View project Modification of Carbon Nanotubes Surface Using Different Oxidizing Agents View project. https://www.researchgate.net/publication/346445002

24 Filip, E. M., Humelnicu, I. v, & Ghirvu, C. I. (2009). Some Aspects of 8-hydroxyquinoline in Solvents (Vol. 17).

25 Amati, M., Belviso, S., Cristinziano, P. L., Minichino, C., Lelj, F., Aiello, I., la Deda, M., & Ghedini, M. (2007). 8-Hydroxyquinoline monomer, water adducts, and dimer. Environmental influences on structure, spectroscopic properties, and relative stability of Cis and Trans conformers. Journal of Physical Chemistry A, 111(51), 13403–13414. https://doi.org/10.1021/jp074510s

26 Bardez, E., Devol, I., Larrey, B., & Valeur, B. (1997). Excited-State Processes in 8-Hydroxyquinoline: Photoinduced Tautomerization and Solvation Effects.

27 Li, Q.-S., & Fang, W.-H. (n.d.). Theoretical studies on structures and reactivity of 8-hydroxyquinoline and its one-water complex in the ground and excited states. www.elsevier.com/locate/cplett

28 Camargo, A. J., Napolitano, H. B., & Zukerman-Schpector, J. (2007). Theoretical investigation of the intramolecular hydrogen bond formation, non-linear optic properties, and electronic absorption spectra of the 8-hydroxiquinoline. Journal of Molecular Structure: THEOCHEM, 816(1–3), 145–151. https://doi.org/10.1016/j.theochem.2007.04.019

29 Karimi Shervedani, R., Rezvaninia, Z., & Sabzyan, H. (2015). Oxinate-Aluminum(III) Nanostructure Assemblies Formed via In-situ and Ex-situ Oxination of Gold-Self-Assembled Monolayers Characterized by Electrochemical, Attenuated Total Reflectance Fourier Transform Infrared Spectroscopy, and X-ray Photoelectron Spectroscopy Methods. Electrochimica Acta, 180, 722–736. https://doi.org/10.1016/j.electacta.2015.07.166

30 Nuha M. Rashed, Sallal A.H. Abdullaha. ((2021) . Metal complexes of mixed ligands novel 2- Thioxoimidazolidine-4- one derivative and glycine Synthesis, characterization and biological activity. Eurasian Journal of Physics, Chemistry and Mathematics

31 Adamolekun, S. (2022). Synthesis, Characterization and Antimicrobial Properties of Mixed Ligand of Sulphamethoxazole and Trimethoprim and Their Manganese (II) and Copper (II) Complexes. In International Journal of Innovative Science and Research Technology (Vol. 7, Issue 2). www.ijisrt.com716

32 Mishra, A. P., Mishra, R., Jain, R., & Gupta, S. (2012). Synthesis of new VO(II), Co(II), Ni(II) and Cu(II) complexes with Isatin-3-chloro-4-floroaniline and 2-pyridinecarboxylidene-4-aminoantipyrine and their antimicrobial studies. Mycobiology, 40(1), 20–26. https://doi.org/10.5941/MYCO.2012.40.1.020

33 Raoof, S. A., Hasan, W. M. G., Aziz, A. A., Saied, S. M., & Saleh, M. Y. (2022). Preparation of New Complexes of Bivalent Manganese, Iron, Cobalt, and Nickel with Mixed Ligands of Ciprofloxacin (Cip) and Metronidazole (Met) or 4-Aminoantipyrine (4AAP) with Study of Their Chemical, Physical Properties and Antibacterial Activity. Egyptian Journal of Chemistry, 65(9), 11–19. https://doi.org/10.21608/EJCHEM.2022.117975.5315

34 Bodkhe, A. S., Patil, S. S., & Shaikh, M. M. (2012). SYNTHESIS, CHARACTERIZATION AND ANTIBACTERIAL STUDIES ON MIXED LIGAND COPPER COMPLEXES WITH POLYDENTATE LIGANDS. Acta Poloniae Pharmaceutica ñ Drug Research, 69(5).

35 Ahmad, W., Khan, S. A., Munawar, K. S., Khalid, A., & Kawanl, S. (2017). Synthesis, characterization and pharmacological evaluation of mixed ligand-metal complexes containing omeprazole and 8-hydroxyquinoline. Tropical Journal of Pharmaceutical Research, 16(5), 1137–1146. https://doi.org/10.4314/tjpr.v16i5.23

36 Khaled M. , Hasan A., Abdulaziz S. A., Ali M.E. (2022) Complexation of Ag(I) with 8-Hydroxyquinoline: Synthesis, Spectral Studies and Antibacterial Activities. Advanced Journal of Chemistry-Section A .Theoretical, Engineering and Applied Chemistry. https://doi.org/10.22034/AJCA.2022.322123.1294

37 Thakur, G. A., & Shaikh, M. M. (2006). SYNTHESIS, CHARACTERIZATION, ANTIBACTERIAL AND CYTOTOXICITY STUDIES ON SOME MIXED LIGAND Th(IV) COMPLEXES. Acta Poloniae Pharmaceutica ñ Drug Research, 63(2), 95–100.

38 Ismael, M., Abdel-Mawgoud, A. M. M., Rabia, M. K., & Abdou, A. (2021). Ni(II) mixed-ligand chelates based on 2-hydroxy-1-naphthaldehyde as antimicrobial agents: Synthesis, characterization, and molecular modeling.

Journal of Molecular Liquids, 330. https://doi.org/10.1016/j.molliq.2021.115611

39 Al-Farhan, B. S., Basha, M. T., Abdel Rahman, L. H., El-Saghier, A. M. M., El-Ezz, D. A., Marzouk, A. A., Shehata, M. R., & Abdalla, E. M. (2021). Synthesis, dft calculations, antiproliferative, bactericidal activity and molecular docking of novel mixed-ligand salen/8-hydroxyquinoline metal complexes. Molecules, 26(16). https://doi.org/10.3390/molecules26164725

40 Nagesh, G. Y., & Mruthyunjayaswamy, B. H. M. (2015). Synthesis, characterization and biological relevance of some metal (II) complexes with oxygen, nitrogen and oxygen (ONO) donor Schiff base ligand derived from thiazole and 2-hydroxy-1-naphthaldehyde. Journal of Molecular Structure, 1085, 198–206. https://doi.org/10.1016/j.molstruc.2014.12.058

41 Khan, H., Badshah, A., Murtaz, G., Said, M., Rehman, Z. U., Neuhausen, C., Todorova, M., Jean-Claude, B. J., & Butler, I. S. (2011). Synthesis, characterization and anticancer studies of mixed ligand dithiocarbamate palladium(II) complexes. European Journal of Medicinal Chemistry, 46(9), 4071–4077. https://doi.org/10.1016/j.ejmech.2011.06.007

42 Fouda, M. F. R., Abd-Elzaher, M. M., Shakdofa, M. M. E., el Saied, F. A., Ayad, M. I., & el Tabl, A. S. (2008). Synthesis and characterization of transition metal complexes of N′-[(1,5-dimethyl-3-oxo-2-phenyl-2,3-dihydro-1H-pyrazol-4-yl)methylene] thiophene-2-carbohydrazide. Transition Metal Chemistry, 33(2), 219–228. https://doi.rg/10.1007/s11243-007-9024-0

43 Bajwan, A., Sharma, P., & Dewan, S. K. (2015). Green Synthesis of Tetraketones Using Barium Chloride. In IISUniv.J.Sc.Tech (Vol. 4, Issue 1).

44 Chniti, S., Nsira, A., Khouaja, S., Mechria, A., Gharbi, R., Msaddek, M., & Lecouvey, M. (2018). Highly diastereoselective synthesis of rigid 3-enamino-1, 5-benzodiazepines. Arkivoc, 2018(5), 283–295. https://doi.org/10.24820/ark.5550190.p010.426

45 Hosny, N. M., Ibrahim, R., & El-Asmy, A. A. (2016). Spectral, thermal, optical and biological studies on (E)-4-[(2-hydroxyphenyl)imino]pentan-2-one and its complexes. Journal of the Serbian Chemical Society, 81(1), 57–66. https://doi.org/10.2298/JSC150201058H

46 Assy, M. G., Mohamed, E. K., Ghoneim, A. A., & Ragab, I. (n.d.). Enamines as a precursor for synthesized of some azoles and azines with expected biological activity.

47 Mansour, S. T., Hashem, A. I., Abd-El-Maksoud, M. A., El-Hussieny, M., El-Makawy, A. I., Abdel-Aziem, S. H., & Soliman, F. M. (2022). The synthesis and antineoplastic activities of thiaziridine, sulfidometylphosphonium, and dithiaphosphitane-sulfide against the Ehrlich ascites carcinoma. Fundamental and Clinical Pharmacology, 36(3), 536–552. https://doi.org/10.1111/fcp.12751

48 Onyenze, U., & Ifeanyi Edozie, O. (2021). Synthesis, Spectroscopic Characterization and Antibactrial Activities of Co(II) Complex of Ofloxacin Drug Mixed with Ascorbic Acid as a Secondary Ligand Synthesis, Spectroscopic Characterization and Antibacterial Activities of Co(II) Complex of Ofloxacin Drug Mixed with Ascorbic Acid as Secondary Ligand. BioScientific Review (BSR), 3, 2021. https://doi.org/10.32350/BSR

49 Kargar, H., Aghaei-Meybodi, F., Elahifard, M. R., Tahir, M. N., Ashfaq, M., & Munawar, K. S. (2021). Some new Cu(II) complexes containing O,N-donor Schiff base ligands derived from 4-aminoantipyrine: synthesis, characterization, crystal structure and substitution effect on antimicrobial activity. Journal of Coordination Chemistry, 74(9–10), 1534–1549. https://doi.org/10.1080/00958972.2021.1900831

50 Kadhom, H. J., Numan, A. T., & Atiyah, E. M. (2022). Characterization of New Ligand for β-enaminone and its Mixed Ligand Complexes with Some Metal Ions and Evaluation of their Biological Activity Synthesis and Characterization of New Ligand for β-enaminone and its Mixed Ligand Complexes with Some Metal Ions and Evaluation of their Biological Activity. International Journal of Drug Delivery Technology, 12(2), 640–647. https://doi.org/10.25258/ijddt.12.2.30

51 Akıncı, A., Celepci, D. B., Karadeniz, L., Korkmaz, N., Aygün, M., & Astley, S. T. (2017). Carboxylate ion dependency in the Cu(II) catalysed asymmetric Henry reaction: Structural characterisation of a tridentate Schiff base complex containing a coordinated carboxylic acid. Applied Organometallic Chemistry, 31(12). https://doi.org/10.1002/aoc.3831

52 Patil, S. S., Tadavi, S. K., Dikundwar, A., & Bendre, R. S. (2022). The transition metal complexes of Fe(II), Ni(II) and Cu(II) derived from phthalazine based ligands: Synthesis, crystal structures and biological activities. Journal of Molecular Structure, 1247. https://doi.org/10.1016/j.molstruc.2021.131293

53 P.Saravana Bhava , P.Tharmaraj , V.Muthuraj , M . Umadevi (2013) Characterization , Biological Screening and DNA Studies of 2- (5 - Mercapto - 1 , 3 , 4 - Oxadiazol - 2 - yl) Phenol Transition Metal (II) Complexes. International Journal Of Engineering And Science Vol.2